Breaking of bonds between a kinesin motor and microtubules causes protein friction

Volker Bormuth[a], Vladimir Varga[a], Jonathon Howard[a] and Erik Schäffer[b*]

[a]Max Planck Institute of Molecular Cell Biology and Genetics,
Photenhauerstraße 108, 01307 Dresden, Germany;
[b]Nanomechanics Group, Biotechnology Center, TU Dresden,
Tatzberg 47-51, 01307 Dresden, Germany

ABSTRACT

Friction limits the operation of macroscopic machines. Using optical tweezers, we showed that friction also limits the operation of molecular machines by measuring the friction between single yeast kinesin-8, Kip3p, and its microtubule track. The protein friction arises from the force necessary to break the adhesive bonds that Kip3p forms with discretely, 8-nm spaced binding sites on its track. A model based on bond rupture dynamics with a single energy barrier described the data. A fluctuation analysis confirmed Kip3p stepping during diffusion. Here, we validate our experimental results and data analysis by a Monte Carlo simulation. Our data have implications for other molecular machines or actively driven proteins, and give further insight into diffusion of proteins along polymers such as microtubules or DNA.

Keywords: Protein friction, optical tweezers, molecular motors, kinesin, bond rupture, force spectroscopy, Monte Carlo simulation, fluctuation analysis

1. INTRODUCTION

Friction within an engine or between a vehicle and its track plays a crucial role in limiting the speed and the efficiency of macroscopic machines. On the molecular scale, friction resists the relative motion of two bodies in contact through adhesive bonds. Friction is the force necessary to deform and break these bonds to allow for movements. When a bond breaks, the stored elastic energy is dissipated. Biological molecular motors such as kinesin are also limited by friction forces. Kinesin binds stereospecifically to discrete sites on a microtubule and in order to move the motor must break this bond to reform a bond at a new location. Using optical tweezers, we measured friction forces between the budding yeast kinesin-8, Kip3p, and its microtubule track.[1]

Kip3p was an ideal model system to study protein friction. When the motor operates in the presence of adenosine diphosphate (ADP), i.e. in the absence of its energy source adenosine triphosphate (ATP), it stays attached to the microtubule in a distinct diffusive state. According to the Einstein relation, the corresponding diffusion coefficient is inversely proportional to the frictional drag coefficient of the motor. To test this relation, we first measured the diffusion coefficient by single-molecule fluorescence tracking. Then, we quantified the friction force using optical tweezers by dragging single motor molecules along the microtubule. We demonstrated the Einstein relation for low speeds and observed a deviation from a linear friction force-velocity relationship at larger speeds. This deviation we explained by a model based on bond rupture dynamics. Furthermore, the friction force depended on the pulling direction reflecting the asymmetry of the polar microtubule filament. The active molecular motor is limited in both speed and efficiency by the presence of this protein friction.

To gain insight into the molecular mechanism of protein diffusion along filaments, we showed that the motor moved by 8-nm diffusive hopping steps. This result we confirmed by (i) the bond-rupture model, (ii) direct observation of steps, and (iii) by a fluctuation analysis. The bond-rupture model was based on a constant force approximation, and the fluctuation analysis requires a Poisson stepper. Here, we validate these two points by a Monte Carlo simulation of the experiment. We show that a correction to the constant force approximation

*Corresponding author: Erik.Schaeffer@biotec.tu-dresden.de

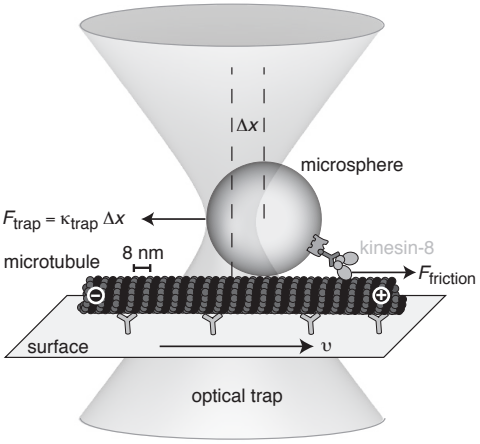

Figure 1. Schematic of the experiment: A kinesin-8-coated microsphere is trapped close to an immobilized microtubule (not drawn to scale). Moving the stage with constant velocity v past the stationary laser drags the microtubule lattice underneath the kinesin-8 molecule. The molecular interaction of the kinesin-8 motor with the microtubule creates a friction force $F_{\text{friction}} = -F_{\text{trap}}$ (neglecting the small hydrodynamic drag arising from the viscosity of the aqueous solution).

due to the presence of force fluctuations describes the simulated data slightly better than the theory without the correction. The fluctuation analysis of the experimental data confirmed the 8-nm steps that we measured at speeds larger than $4\,\mu$m/s, but underestimated the step size at lower speeds. We argue here that the underestimate arises because the loading rate of the optical trap depletes the population of long-lived states. First we summarize the experimental procedure used to measure protein friction, then we describe the simulation procedure, followed by the presentation of the simulated data which we compare to the experimental results.

2. EXPERIMENTAL PROCEDURE

With an optical tweezers,[1–6] we trapped polystyrene microspheres (500 nm in diameter) functionalized with single yeast kinesin-8 (Kip3p) molecules[7–9] and dragged them over microtubules (Fig. 1). We placed the microspheres over surface-immobilized microtubules such that the Kip3p molecules could interact with the microtubule.[10,11] The interaction was diffusive, since the surrounding solution contained ADP which cannot be used as a fuel for the motor. Then we moved the stage with constant speed forwards and backwards along the axis of the microtubule resulting in a relative movement of the laser and the trapped microsphere with respect to the microtubule. After binding of the Kip3p molecule to the microtubule in its diffusive state, the microsphere was displaced relative to the trap center and the molecule dragged along the microtubule with an on average constant force. The force that was necessary to drag the molecule with constant speed was a direct measure of the friction between the single kinesin molecule and its microtubule track. We performed the experiment for different drag speeds and analyzed the data for dragging towards the microtubule plus- and minus-end independently. On the single-molecule level, we explained the measured friction and the observed diffusion by bond rupture dynamics.

3. SIMULATION

In the absence of an external force the molecular motor diffused along the microtubule lattice. The diffusive motion can be modelled as a Poission stepper between discrete binding sites, with equal probability of making a forward and a backward step of size δ. In a single-step Poission process, the probability of making a step is independent of the occurrence of the previous step resulting in an exponential probability distribution of the dwell time occurence between steps:

$$P(\tau) = e^{-(k_+ + k_-)\tau}, \tag{1}$$

where $k_+ = k_- = k_0 = \langle\tau\rangle^{-1}$ is the rate of forward or backward stepping and $\langle\tau\rangle$ is the average dwell time. The distribution gives the probability that no step occurred during the time interval τ. The probability of a step in a time interval Δt is then $P_{\text{step}} = 1 - P(\Delta t)$. To simulate the step-wise movement of the molecule, we

calculated in discrete time steps separated by the time interval $\Delta t \ll (k_f + k_b)^{-1}$ a random number, r, between 0 and 1. For $r < P_{\text{step}} = 1 - e^{-2k_0\Delta t}$ we increased or decreased with equal probability of forward and backward steps, $P_f = P_b = 0.5$, the molecule position, x, by δ resulting in a random walk with exponential dwell time distribution.

In the experiment using the optical tweezers, we dragged—with constant velocity—the diffusing molecule via a microsphere-handle along a microtubule. As long as the molecule was detached from the microtubule the microsphere moved together with the center of the optical trap. After binding of the molecule onto the microtubule in its diffusive state the friction force between the molecule and the microtubule slowed the microsphere down, thus displacing it out of the trap, leading to the application of a force (Fig. 1),

$$F = -F_{\text{friction}} = F_{\text{trap}} = \kappa_{\text{trap}}\Delta x, \tag{2}$$

where κ_{trap} is the trap stiffness and, Δx is the displacement relative to the trap center. When the trap force was on average balanced by the friction force, the microsphere moved with the same speed as the trap but lagged behind the trap with an on average constant offset.

The force applied by the optical tweezers biased the diffusion of the molecule by changing the forward and the backward stepping rate according to an Arrhenius-like theory

$$k_\pm = k_0 e^{\pm\frac{1}{2}F\delta/k_BT}. \tag{3}$$

Note that here we did not consider an asymmetric interaction potential.[1] Inserting Eq. 3 into Eq. 1 gives the force-dependent dwell time distribution with the probability of a backward step $P_b = 1 - P_f = \frac{k_-}{k_+ + k_-}$. For the simulation we created two variables, one for the molecule position, x, and one for the trap position, x_{trap}. Starting with both variables at zero, we increased x_{trap} every simulation time interval Δt by $v\Delta t$, with v being the drag speed. After each update of the trap position, we (i) calculated the applied force $F = \kappa_{\text{trap}}(x_{\text{trap}} - x)$ on the molecule, (ii) evaluated the force-dependent stepping probability, and (iii) in case of the occurrence of a step, increased or decreased the molecule position x by the step size δ.

4. RESULTS

To compare the simulation with the experimental results, we chose parameters closely matching those of the experiment. In particular, we used for the simulation step time $\Delta t = 5\,\mu$s which corresponds to five times the experimental sampling rate. The step size was $\delta = 8.2\,$nm reflecting the periodicity of the microtubule lattice.[14] The diffusion coefficient was $D = \delta^2 k_0 = 5400\,\text{nm}^2/\text{s}$ corresponding to a zero-force stepping rate of $k_0 \approx 80\,\text{s}^{-1}$ and a frictional drag coefficient $\gamma = k_\text{B}T/D \approx 0.76\,\mu$Ns/m. The trap stiffness was about the same as the one in the experiments $\kappa_{\text{trap}}^{\text{exp}} = 0.038\,$pN/nm unless mentioned otherwise.

4.1 Force-velocity relation

Plotting the simulated trap force over time showed—after a transient response—a plateau of the trap force that increased for larger drag speeds (Fig. 2A). The average plateau value is plotted versus the drag speed in Fig. 2B. The error bars indicate the standard error of the mean (SEM) calculated with the method from H. Flyvbjerg[12] to estimate the error in correlated data. The standard deviation of the force signal was about 0.4 pN for $\kappa_{\text{trap}}^{\text{exp}} = 0.038\,$pN/nm and did not vary with velocity. The simulated force-velocity data points closely resemble the experimental results.[1] The black line in Fig. 2B is the friction force-velocity relation according to our theory

$$v = \delta(k_+ - k_-) \tag{4}$$

with k_+ and k_- being force dependent according to Eq. 3.

The theory assumes a constant trap force without force fluctuations. Force fluctuations lead to a correction term (see Eq. S3 in supplementary material of Bormuth *et al.*[1]). With the correction the simulated data are slightly better described (dotted line in Fig. 2B). As a control, we verified that the average force did not vary with trap stiffness in the range of the experimentally used values (inset Fig. 2B). This indicates that there is no loading-rate dependence of the bond-rupture force for a sufficiently low trap stiffness. For a large trap stiffness, the simulated average force decreased while the standard deviation increased (solid lines through data points in the inset of Fig. 2B).

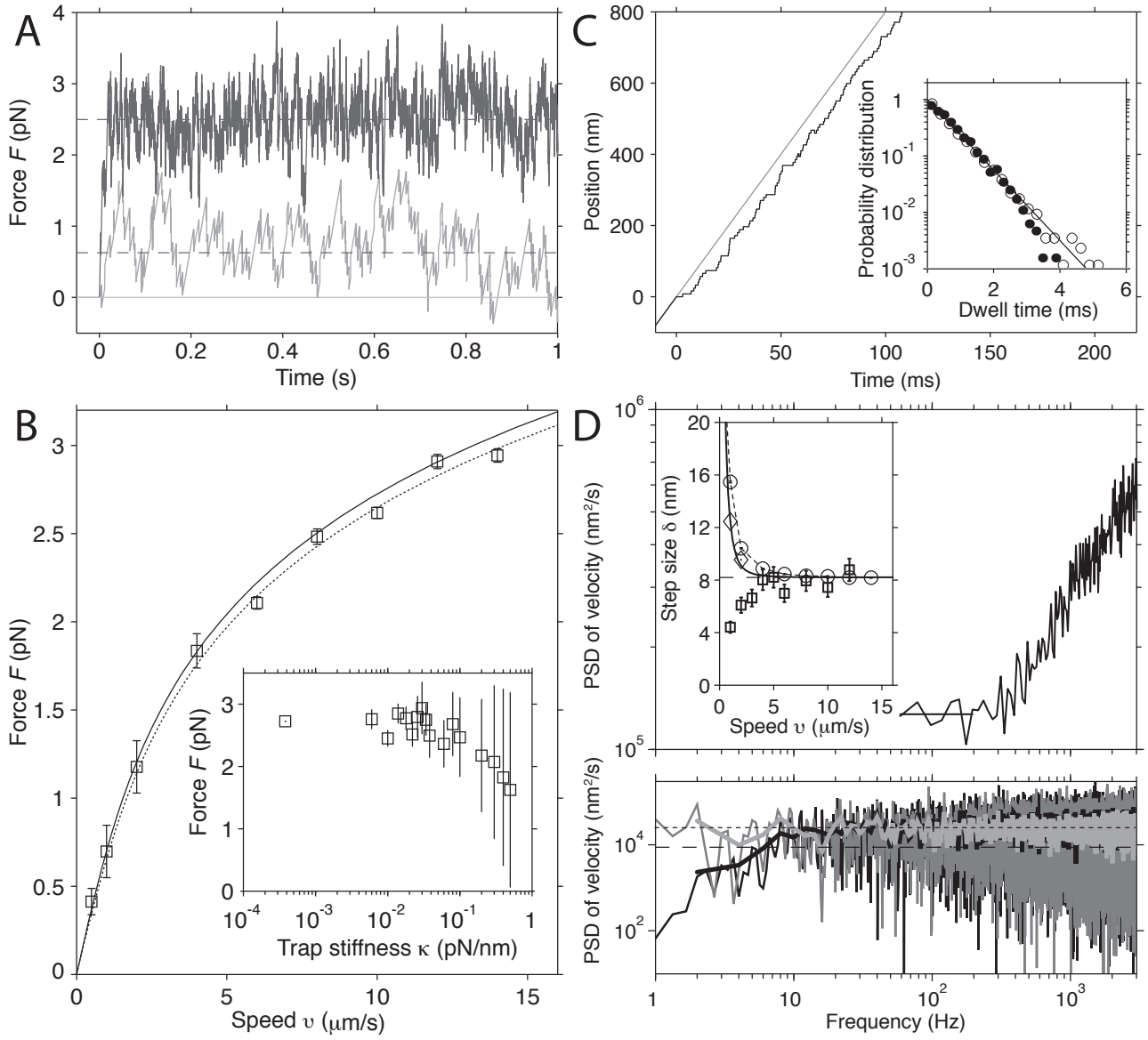

Figure 2. **A** Friction force vs. time as a result of the simulation [$v = 1\,\mu$m/s (light gray), $v = 8\,\mu$m/s (dark gray)]. The dashed lines indicate the averages of the force plateaus. **B** Friction force-velocity relationship: The average force plateau height is plotted versus the drag speed. The error bars—the standard error of the mean (SEM)—were determined by a "blocking" method.[12] The bond-rupture model with constant force approximation (solid line) and correction (dotted line) describe the data well within the error bars. Inset: Mean force as a function of trap stiffness for $v = 10\,\mu$m/s. SEM (not shown) are about the size of the symbols; vertical lines depict the standard deviation. **C** Stepwise motion of the motor position (black) and trap position (gray) as a function of time. Inset: Probability distribution for dwell-time occurrence for $v = 12\,\mu$m/s with $\kappa_{\mathrm{trap}}^{\mathrm{exp}} = 0.038\,$pN/nm (solid circles) and $\kappa_{\mathrm{trap}}^{\mathrm{low}} = 0.00038\,$pN/nm (open circles). Equation 1 (solid line) was fitted using a scaling factor to the latter data set with the rate fixed to the one expected. **D** Fluctuation analysis. Top: Experimental velocity power spectral density (PSD) trace for $v = 8\,\mu$m/s with the solid straight line indicating the plateau average. Inset: Step size as a function of drag speed [experimental data (squares), simulation evaluated at high frequencies and $\kappa_{\mathrm{trap}}^{\mathrm{exp}}$ (circles and dotted line) and $\kappa_{\mathrm{trap}}^{\mathrm{low}}$ (diamonds), theoretical curve with backward steps[13] (solid line)]. Bottom: Velocity PSD based on simulation at $v = 1\,\mu$m/s for $\kappa_{\mathrm{trap}}^{\mathrm{exp}}$ (black) and $\kappa_{\mathrm{trap}}^{\mathrm{low}}$ (gray); thick lines are averaged PSDs. Dashed lines indicate plateau heights corresponding to about 12 nm (short dash) and 4 nm (long dash) step size.

4.2 Fluctuation analysis

We used a fluctuation analysis[1,15] to objectively measure the diffusive hopping-step size using all our (noisy) experimental data. This analysis is valid for a single-step random process with an exponential dwell-time distribution without backward steps. We observed[1] a decrease in step size for $v < 4\,\mu$m/s (squares, Fig. 2D, inset), which suggested that several rate-limiting processes at low forces exist, as has been reported for kinesin-1.[16] Therefore, we simulated the data to test whether there would be other explanations for the decrease in step size.

Figure 2C shows a typical time trace of the simulated movement of the dragged molecule. The 8 nm steps are clearly visible in the simulation because we did not add Brownian noise to the positional data. This Brownian noise obscured the steps in the experiments requiring the fluctuation-based analysis. The inset shows a nearly exponential probability distribution of dwell time occurrence (the deviations are discussed below). Taking the time derivative of the position data, results in randomly distributed delta functions occurring at the times when the motor stepped. This random distribution leads to a flat velocity power spectral density (PSD), i.e. white noise, with an average plateau height of $p = 2v\delta$ (Fig. 2D, bottom). Since the drag speed v is known precisely this equation can be used to determine the step size δ (Fig. 2D, inset). Due to the positional Brownian noise in the experiment, the velocity PSD increased quadratically with frequency for high frequencies above a characteristic frequency f_c^{noise} (≈ 300 Hz in Fig. 2D, top). Thus, the plateau below this frequency needs to be evaluated.

A theory with backward steps[13] predicts an apparent increase in step size for small drag speeds (solid line, Fig. 2D, inset). The velocity PSDs based on the simulations (Fig. 2D, bottom) indeed confirm this increase when the step size is based on the average PSD at high frequencies (above 1 kHz). However, when the average is taken at low frequencies, the step size is underestimated since the velocity PSD decreased for low frequencies. When reducing the trap stiffness 100-fold, the decrease in the velocity PSD at low frequencies disappeared and the theoretically predicated increase in step size is recovered by the simulation even when the PSD is evaluated at low frequencies.

5. DISCUSSION

The simulation validated our experimental data analysis. Furthermore, it gave insight into how the trap stiffness affects the dwell time distribution of the steps and the force fluctuations. With respect to the bond rupture model, we confirmed that the *average* force was independent of the trap stiffness for a sufficiently low trap stiffness. Thus, for the trap stiffness used in the experiments, there was no loading rate dependence for the rupture of a single bond requiring no further correction to the model with that respect (see Sect. 9.1 in Bormuth *et al.*[1]). However, with increasing trap stiffness, the *fluctuations* in force increased. Qualitatively, the fluctuations in position due to the diffusive nature of the interaction remain nearly constant for a given pulling speed. Since the force fluctuations are the product of the positional fluctuations with the trap stiffness, an increase of the latter also results in an increase of the force fluctuations.

Fluctuations in the force affect the force-dependent hopping rates. Since the speed (Eq. 4) is based on the average rates and the force occurs in the exponential, the fluctuations do not simply average out but lead to a correction term (Eq. S3 in Bormuth *et al.*[1]). This correction increases the rates with increasing force fluctuations. Thus, for a given speed, i.e. a given rate, the *average* force has to decrease when the force fluctuations increase. Since fluctuations were present in both the experimental and simulated data, this correction (dotted line in Fig. 2B) therefore led to a better description of the data.

The second effect of the trap stiffness is that it changes the dwell time distribution. Since the optical trap is constantly moving, a long dwell or pause of a motor before a step results in more loading, i.e. a higher force acting on the motor. Since the loading rate, $v\kappa_{\text{trap}}$, increases with increasing trap stiffness, the probability of long dwell times is increasingly reduced with a higher trap stiffness. This effect we observed in the probability distribution for dwell-time occurrence (inset Fig. 2C).

The change in the probability distribution for the dwell-time occurrence affected the fluctuation analysis. We can define a characteristic frequency at which the loading rate has increased the hopping rate e-fold. This occurs at a force increase due to a fluctuation of $\Delta F = 2k_{\text{B}}T/\delta$ which corresponds to a displacement of $\Delta x = \Delta F/\kappa_{\text{trap}}$ and a lag time, τ_c, or characteristic frequency, f_c^{trap}, of $\tau_c^{-1} = f_c^{\text{trap}} = v/\Delta x = \kappa_{\text{trap}}\delta v/(2k_{\text{B}}T)$. Note that additional compliance due to a molecular linker—not simulated here—between the microsphere and the molecular

motor in the experiments (Fig. 1) might change the value of this frequency. For frequencies $f \lesssim f_c^{\mathrm{trap}}$ (longer lag times than τ_c), we expected a reduced power spectral density. The velocity PSD in the bottom of Fig. 2D indeed showed such a drop in power for low frequencies. This drop disappeared (moved to much lower frequencies) when the trap stiffness was lowered 100-fold. Thus, ideally drag experiments should be performed with the lowest possible trap stiffness.

The decrease in the low-frequency power spectral density leads to an under-estimation of the step size based on the fluctuation analysis if the frequencies below f_c^{trap} are included in the analysis. If the trap stiffness was sufficiently low, exponential dwell time distributions and flat PSDs were recovered leading to the correct step size (inset Fig. 2D). Also correct values were obtained at very high frequencies which were, however, inaccessible in the experimental data due to Brownian noise in the position data. In the experiments for $v \geq 4\,\mu$m/s, the plateaus were analyzed between the lower—f_c^{trap} due the trap stiffness—and upper—f_c^{noise} due to Brownian noise—corner frequencies where the plateau was flat. This led to the correct estimate of the step size. For $v < 4\,\mu$m/s, we found $f_c^{\mathrm{trap}} \approx f_c^{\mathrm{noise}}$ which means that there was no flat plateau region leading to an under-estimate of the step size. Thus, the simulation suggests that the apparent decrease in step-size is due to the finite stiffness of the trap and not due to a multi-step process.[1,15]

ACKNOWLEDGMENTS

We thank Ralf Seidel for discussions. The work was supported by the Deutsche Forschungsgemeinschaft (Emmy Noether Program), the Max Planck Society, and the Technische Universität Dresden.

AUTHOR CONTRIBUTION

V.B. J.H. and E.S. designed research; V.B. J.H. and E.S. performed research; V.B., and E.S. analyzed data; V.V. and J.H. provided advice; and V.B. and E.S. wrote the paper.

REFERENCES

[1] Bormuth, V., Varga, V., Howard, J., and Schäffer, E., "Protein friction limits diffusive and directed movements of kinesin motors on microtubules," *Science* **325**, 870–873 (2009).

[2] Schäffer, E., Nørrelykke, S. F., and Howard, J., "Surface forces and drag coefficients of microspheres near a plane surface measured with optical tweezers," *Langmuir* **23**(7), 3654–3665 (2007).

[3] Bormuth, V., Howard, J., and Schäffer, E., "LED illumination for video-enhanced DIC imaging of single microtubules," *J. Microsc.* **226**(1), 1–5 (2007).

[4] Bormuth, V., Jannasch, A., Ander, M., van Kats, C. M., van Blaaderen, A., Howard, J., and Schaffer, E., "Optical trapping of coated microspheres," *Opt. Express* **16**(18), 13831–13844 (2008).

[5] Jannasch, A., Bormuth, V., van Kats, C. M., van Blaaderen, A., Howard, J., and Schaffer, E., "Coated microspheres as enhanced probes for optical trapping," *Proc. SPIE* , 70382B (8 pp.) (2008).

[6] Mahamdeh, M. and Schäffer, E., "Optical tweezers with millikelvin precision of temperature-controlled objectives and base-pair resolution," *Opt. Express* **17**, 17190–17199 (2009).

[7] Bormuth, V., Zörgiebel, F., Schäffer, E., and Howard, J., "Functional surface-attachment in a sandwich geometry of GFP-labeled motor proteins," *Single Molecule Enzymology* (2010). In print.

[8] Varga, V., Helenius, J., Tanaka, K., Hyman, A. A., Tanaka, T. U., and Howard, J., "Yeast kinesin-8 depolymerizes microtubules in a length-dependent manner," *Nat. Cell Biol.* **8**(9), 957–962 (2006).

[9] Varga, V., Leduc, C., Bormuth, V., Diez, S., and Howard, J., "Kinesin-8 motors act cooperatively to mediate length-dependent microtubule depolymerization," *Cell* **138**, 1174–1183 (2009).

[10] Gell, C., Bormuth, V., Brouhard, G. J., Cohen, D. N., Diez, S., Friel, C. T., Helenius, J., Nitzsche, B., Petzold, H., Ribbe, J., Schäffer, E., Stear, J. H., Trushko, A., Varga, V., Widlund, P. O., Zanic, M., and Howard, J., "Microtubule dynamics reconstituted in vitro and imaged by single-molecule fluorescence microscopy," *Methods Cell Biol.* **95**, 221–245 (2010).

[11] Nitzsche, B., Bormuth, V., Bräuer, C., Howard, J., Ionov, L., Kerssemakers, J. W. J., Korten, T., Leduc, C., Ruhnow, F., and Diez, S., "Microtubule dynamics reconstituted in vitro and imaged by single-molecule fluorescence microscopy," *Methods Cell Biol.* **95**, 247–271 (2010).

[12] Flyvbjerg, H. and Petersen, H. G., "Error-estimates on averages of correlated data," *J. Chem. Phys.* **91**(1), 461–466 (1989).

[13] Thomas, N., Imafuku, Y., and Tawada, K., "Molecular motors: thermodynamics and the random walk," *Proc. R. Soc. Lond., B* **268**(1481), 2113–2122 (2001).

[14] Howard, J., [*Motor Proteins and the Cytoskeleton*], Sinauer Associates, Sunderland, MA (2001).

[15] Charvin, G., Bensimon, D., and Croquette, V., "On the relation between noise spectra and the distribution of time between steps for single molecular motors," *Single Mol.* **3**(1), 43–48 (2002).

[16] Svoboda, K., Mitra, P. P., and Block, S. M., "Fluctuation analysis of motor protein movement and single enzyme-kinetics," *Proc. Natl. Acad. Sci. U. S. A.* **91**(25), 11782–11786 (1994).